

to them in the next section, followed by sections of experiments and results and discussion.

Theory

General Remarks and Basic Assumptions. We first consider LRP of dissociation–combination (DC) type including an initiating adduct P_0-X and monomer but no persistent radical X^\bullet at $t = 0$. When a polymerization run is started by allowing P_0-X to dissociate, the same number of P_0^\bullet and X^\bullet will be produced in a unit time, and $[P_0^\bullet]$ and $[X^\bullet]$ will linearly increase with time t . The radical P_0^\bullet may add to the monomer to give a polymer radical P^\bullet . The radicals P_0^\bullet and P^\bullet are assumed to be kinetically identical and both will be written P^\bullet , unless otherwise noted. This approximation is justified when P_0-X is a polymer adduct, as in this work. As $[P^\bullet]$ and $[X^\bullet]$ increase to a certain level, the reactions among P^\bullet and X^\bullet will become significant. Since the bimolecular termination of P^\bullet results in a decrease of $[P^\bullet]$ but not of $[X^\bullet]$, $[X^\bullet]$ will steadily increase, and the reaction between X^\bullet and P^\bullet will become more and more important, leading to a balance of the rate of deactivation, $k_t[P^\bullet][X^\bullet]$, with that of activation, $k_d[P-X]$. Namely, the quasi-equilibrium

$$k_d[P-X] = k_c[P^\bullet][X^\bullet] \quad (1)$$

will hold there. On the other hand, in the time range where the quasi-equilibrium holds, $[P^\bullet]$ must be a decreasing function of time, since the self-termination of P^\bullet continues to occur. This means that $[P^\bullet]$, which linearly increases with t at the onset of polymerization, will turn to a decreasing function (actually $[P^\bullet]$ decays in a power law; see below), going through a maximum. The role of conventional initiation, whose rate R_i is usually much smaller than $k_d[P-X]$, is unimportant during an early stage of polymerization but becomes crucially important when the concentration of P^\bullet comes down to the level such that the equality of initiation and termination rates holds:¹²

$$R_i = k_t[P^\bullet]^2 \quad (2)$$

where k_t is the termination rate constant. This realizes a stationary concentration of P^\bullet and hence a stationary rate of polymerization in LRP as in conventional FRP. If the stable radical X^\bullet is present at $t = 0$, it obviously shortens the time to reach the quasi-equilibrium. Of course, too much of X^\bullet present at $t = 0$ can make the equilibrium value of $[P^\bullet]$ too low or the polymerization rate impractically too low (eq 1).

The mentioned work of X^\bullet to adjust the radical concentrations so as to produce a high preference for cross-combinations was originally recognized in the chemistry of low-mass compounds and termed the persistent radical effect (PRE).^{7–10} In the field of polymerization, such work of persistent radicals was clearly recognized by Johnson et al.¹¹ in their simulation work and subsequently by Fukuda et al.¹² and Greszta and Matyjaszewski,¹³ and clear experimental evidence was presented for the inequality^{12,14} $[X^\bullet] \gg [P^\bullet]$ and the quasi-equilibrium in eq 1.¹² Subsequently, Fischer^{15,16} made a detailed theoretical analysis on the PRE in polymerization. For more details about PRE, the readers are referred to the recent excellent review by Fischer.¹⁷

In the following, we consider systems that meet the three requirements, i.e., (1) the quasi-equilibrium is

reached so fast that the preequilibrium stage has no significant effect on the polymerization kinetics and polymer structure, (2) the main body of polymerization occurs in the time range of quasi-equilibrium, and (3) the cumulative numbers of dead chains (by termination) and initiated chains (by conventional initiation) are sufficiently small compared to the number of dormant chains, or in other words, the equality $[P-X] = [P-X]_0$ ($= [P_0-X]_0$) approximately holds throughout the polymerization. (More specific conditions that the rate constants should obey to meet these requirements and given elsewhere,^{15–17} and it may be easily confirmed that the system to be experimentally studied in the next section meets them.)

Rate Equations. Setting the above statements into equations, we have

$$d[X^\bullet]/dt = k_d[P-X] - k_c[P^\bullet][X^\bullet] \quad (3)$$

$$d[P^\bullet]/dt = k_d[P-X] - k_c[P^\bullet][X^\bullet] + R_i - k_t[P^\bullet]^2 \quad (4)$$

where the rate of conventional initiation R_i is assumed to be constant. All possible reactions other than those indicated in eqs 3 and 4 (and propagation) are neglected, and all the rate constants are assumed to be independent of chain length and other factors. Under these and already noted conditions, eqs 3 and 4 can be approximately solved analytically. Namely, taking the difference of eq 3 minus eq 4, neglecting $d[P^\bullet]/dt$ compared to $d[X^\bullet]/dt$, and approximating $[P^\bullet]$ by

$$[P^\bullet] = K[P-X]_0/[X^\bullet] \quad (5)$$

$$K = k_d/k_c \quad (6)$$

we have the differential equation

$$d[X^\bullet]/dt = k_t(K[P-X]_0/[X^\bullet])^2 - R_i \quad (7)$$

which is readily solved to yield^{18,19}

$$\ln\{[(1+z)/(1-z)][(1-z_0)/(1+z_0)]\} - 2(z-z_0) = bt \quad (8)$$

$$z = \{R_i/(k_t K^2 [P-X]_0^2)\}^{1/2} [X^\bullet] \quad (9)$$

$$b = 2R_i^{3/2}/(k_t K^2 [P-X]_0^2)^{1/2} \quad (10)$$

Here z_0 is the value of z at $t = 0$ ($[X^\bullet] = [X^\bullet]_0$ at $t = 0$). The polymerization rate R_p is obtained from $R_p = -d[M]/dt = k_p[P^\bullet][M]$ with $[P^\bullet]$ given by eq 5 and k_p being the propagation rate constant.

Several special cases are particularly noteworthy in relation to the present work. When $R_i = 0$, eq 8 reduces to²⁰

$$[X^\bullet]^3 = [X^\bullet]_0^3 + 3k_t K^2 [P-X]_0^2 t \quad (R_i = 0) \quad (11)$$

which gives the rate eq 12:

$$\ln([M]_0/[M]) = \{k_p/(2k_t K [P-X]_0)\} \{ (3k_t K^2 [P-X]_0^2 t + [X^\bullet]_0^{2/3} - [X^\bullet]_0^2) \} \quad (R_i = 0) \quad (12)$$

Equation 12 further reduces to two interesting limiting cases. When $[X^\bullet]_0 = 0$, it gives the power-law eq 13 first derived by Fischer¹⁵ using a dimensional analysis and

subsequently by us^{21} using the present method:

$$\ln([M]_0/[M]) = {}^{3/2}k_p(K[P-X]_0/3k_t)^{1/3}t^{2/3} \quad (R_i = [X^*]_0 = 0) \quad (13)$$

In the other limit of large $[X^*]_0$ ($[X^*]_0 \gg (3k_tK^2[P-X]_0^2t)^{1/3}$), eq 12 reduces to²⁰

$$\ln([M]_0/[M]) = (k_pK[P-X]_0/[X^*]_0)t \quad (R_i = 0, [X^*]_0 \gg 0) \quad (14)$$

In this limit, the conversion index $\ln([M]_0/[M])$ is first-order in t . On the other hand, when $R_i > 0$ and $bt \gg 1$, eq 8 reduces to $z = 1$, i.e., to eq 2, and the rate equation reads²²

$$\ln([M]_0/[M]) = k_p(R_i/k_t)^{1/2}t \quad (R_i > 0, bt \gg 1) \quad (15)$$

In this limit, too, the conversion index is linear in t .

Polydispersity Equations. We define the polydispersity factor Y by

$$Y = (M_w/M_n) - 1 \quad (16)$$

where M_w and M_n are the weight- and number-average molecular weights, respectively, and define the polydispersity factor of the "grown portion" of the chain, Y_B , by

$$Y = w_A^2 Y_A + w_B^2 Y_B \quad (17)$$

Here Y and Y_A are the polydispersity factors of the whole chain and the initiating portion of the chain, respectively, and w_A and w_B are the weight fractions of the initiating and grown portions of the chain ($w_A + w_B = 1$). Equation 17 is based on the assumption that the lengths of the A and B portions of the chain are uncorrelated with each other^{23,24} or, equivalently, that the rate constants are independent of chain length.

The polydispersity factor of the system corresponding to the power-law equation has been derived by Fischer,^{16a} which, in the form of Y_B , reads

$$[Y_B - (1/x_{n,B})]^{-1} = k_d t / G(c) \quad (R_i = [X^*]_0 = 0) \quad (18)$$

$$G(c) = ({}^{2/3}c^2)u^3 \int_0^u \exp(-x^2) dx \quad (19)$$

where $u = [-2 \ln(1 - c)]^{1/2}$, c is the conversion, and $x_{n,B}$ is the number-average degree of polymerization of the grown portion of the chain. For small c , eq 18 reduces to

$$[Y_B - (1/x_{n,B})]^{-1} = {}^{3/8}k_d t \quad (R_i = [X^*]_0 = 0) \quad (20)$$

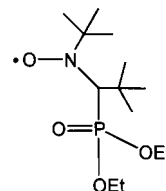
On the other hand, when the radical concentration $[P^*]$ is constant due either to large $[X^*]_0$ (eq 14) or to large bt (eq 15), Y_B is given by^{23a,24}

$$[Y_B - (1/x_{n,B})]^{-1} = k_d t / F(c) \quad (\text{stationary state}) \quad (21)$$

$$F(c) = (1 - 2c^{-1}) \ln(1 - c) \quad (22)$$

which, for small c , reduces to

$$[Y_B - (1/x_{n,B})]^{-1} = {}^{1/2}k_d t \quad (\text{stationary state}) \quad (23)$$



DEPN

Figure 1. Structure of DEPNO.

Thus, the theory predicts that at the same polymerization time, the polydispersity factor, or, more precisely, $Y_B - (1/x_{n,B})$ is smaller in the stationary-state system than in the power-law-type system. Obviously, the polymerization rate is the largest for systems with a conventional initiation and the smallest for systems without it but with a nonzero value of $[X^*]_0$. Since the above discussion on polydispersity neglects the contribution of terminated and (conventionally) initiated chains, it is strictly valid only for small t or small c (but of course not for too small t or c where the quasi-equilibrium is still not established). In other words, experiments to be designed to verify these theoretical predictions must be designed so strictly.

Experimental Section

Materials. Commercially available styrene and benzoyl peroxide (BPO) were purified by fractional distillation and recrystallization from methanol, respectively. *N-tert*-Butyl-1-diethylphosphono-2,2-dimethylpropyl nitroxide (DEPN; Figure 1) was prepared according to Tordo et al.⁴ A polystyrene (PS)–DEPN adduct ($M_n = 2200$ and $M_w/M_n = 1.13$) was obtained as described previously,²⁵ which was used as an initiating adduct P_0-X in the following experiments. A chain extension test²⁶ showed that this polymer contains 5% of potentially inactive species (without a DEPNO moiety at the chain end). *All the experimental data presented below have been corrected for these impurities.*

Kinetic Analysis of Polymerization. A styrene solution of P_0-X (25 mM), DEPNO (0 or 1.8 mM), and BPO (0 or 4.7 mM) in a glass tube was degassed by three freeze–pump–thaw cycles, sealed off under vacuum, and heated at 80 °C for a prescribed time. The reaction mixture was diluted with tetrahydrofuran (THF) to a known concentration and analyzed by gel permeation chromatography (GPC).

GPC. The GPC analysis was made on a Tosoh HLC-802 UR high-speed liquid chromatograph equipped with Tosoh gel columns G2500H, G3000H, and G4000H (Tokyo, Japan). THF was used as eluent (40 °C). The column system was calibrated with Tosoh standard PSs. A known amount of sample solution (of a known concentration) was injected in the column system, and detection and quantification were made with a Tosoh differential refractometer RI-8020 calibrated with known concentrations of PSs in THF.

Examples of GPC curves are given in Figure 2. In both the absence (Figure 2a) and presence (Figure 2b) of BPO, each chromatogram for $t > 0$ clearly consists of two components, the initiating portion (portion A) and the grown portion (portion B). Since we know the complete chromatogram of the initiating adduct (the one for $t = 0$), we can easily compute Y_B from the overall chromatogram, according to eq 17. Despite the extremely low conversion regions studied in this work (see later), the Y_B values determined in this way are sufficiently accurate, because the portions B are sufficiently large compared with the portion A, as Figure 2 indicates.

Results and Discussion

Theoretical relations to be experimentally studied here include the rate equations 13, 14, and 15 and the polydispersity formulas 20 and 23. The stationary-state

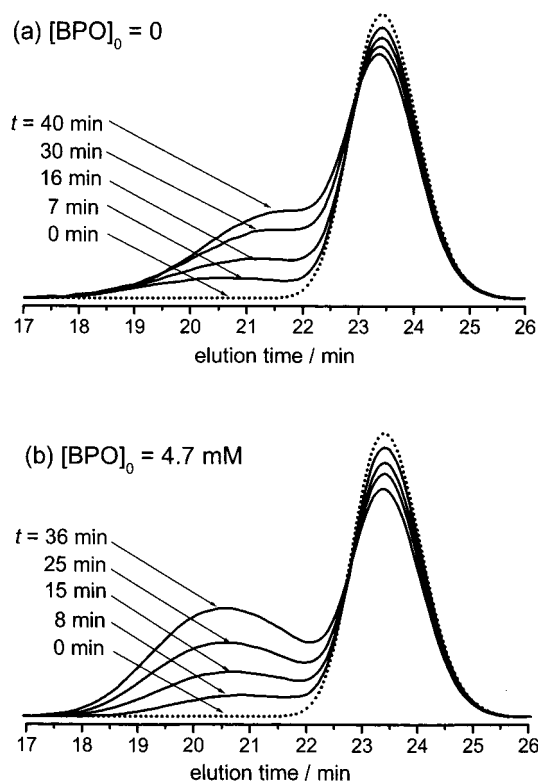


Figure 2. GPC chromatograms for the styrene/PS-DEPN-(P₀-X)/(BPO) systems (80 °C): [P₀-X]₀ = 25 mM; [BPO]₀ = (a) 0 and (b) 4.7 mM.

Table 1. Kinetic Parameters Used in This Work (80 °C)

parameter	value	ref
$k_{i,th}$ (M ⁻² s ⁻¹)	4.5×10^{-12}	37
$k_{i,BPO}$ (s ⁻¹)	6.7×10^{-5}	38
k_p (M ⁻¹ s ⁻¹)	650	39
k_t (M ⁻¹ s ⁻¹)	3.0×10^8 ^a	this work
k_d (s ⁻¹)	1.16×10^{-4}	25
K (M)	1.7×10^{-10}	this work

^a Applicable for an early-stage polymerization with P₀-X (M_n = 2200, M_w/M_n = 1.13).

equation 15 was previously verified for the TEMPO (2,2,6,6-tetramethylpiperidiny-1-oxy)-mediated LRP of styrene at high temperatures where the thermal initiation brought about the stationarity of polymerization rate,^{12,22,27} and the corresponding polydispersity equation 23 was also verified for the TEMPO system.^{23a,24} The power-law behavior predicted by eq 13 was observed by us²¹ for the DBN (di-*tert*-butyl nitroxide)-mediated LRP of a sugar-carrying styrene derivative and subsequently by Boutevin et al.²⁸ in a more quantitative fashion for the DEPN-mediated LRP of styrene. The stationary-state behavior indicated by eq 14 was observed in DC-type^{5,6,29-32} as well as AT-type³³⁻³⁶ LRPs, and this relation was used to determine the equilibrium constant K . The polydispersity equations 20 (for the power-law system) and 23 (for the large-[X]₀ system) have never been experimentally studied before.

Rate Constants. The parameters used in this work are listed in Table 1, where $k_{i,th}$ ³⁷ and $k_{i,BPO}$ ³⁸ are the rate constant of thermal initiation and that of the initiation due to BPO decomposition (with the initiation efficiency included). The initiation rate R_i , which is assumed here to be constant, is given by

$$R_i = k_{i,th}[M]_0^3 + k_{i,BPO}[BPO]_0 \quad (24)$$

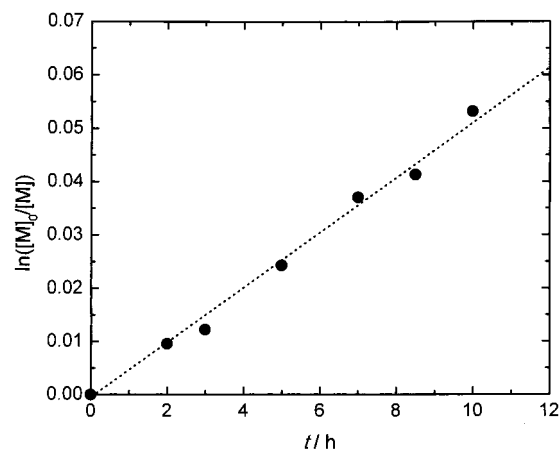


Figure 3. Plot of $\ln([M]_0/[M])$ vs t for the styrene/PS-DEPN-(P₀-X)/DEPN system (80 °C): [P₀-X]₀ = 25 mM; [DEPN]₀ = 1.8 mM. The dotted line is the best-fit representation of the data points.

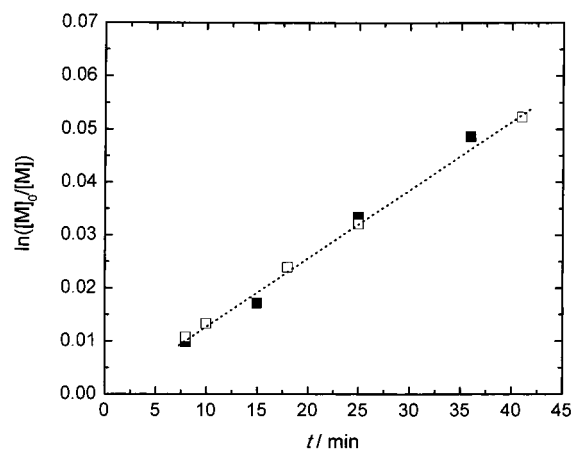


Figure 4. Plot of $\ln([M]_0/[M])$ vs t for the styrene/PS-DEPN-(P₀-X)/BPO system (80 °C): [P₀-X]₀ = 25 mM; [BPO]₀ = 4.7 mM. The dotted line is the best-fit linear representation of the duplicated experiment (■, □).

with $[M]_0 = 7.7$ M and $[BPO]_0 = 4.7$ mM or zero in this study. The k_p is the IUPAC benchmark value,³⁹ and the k_d is the one previously determined by the GPC curve-resolution method.²⁵ Since there are no reported data of K and k_t applicable to the present analysis, we estimated them from the stationary-state experiments.

Namely, to estimate K , we carried out the polymerization of styrene including the PS-DEPN adduct ([P₀-X]₀ = 25 mM: see Experimental Section) and a sufficiently large amount of DEPN at $t = 0$ ([X]₀ = 1.8 mM). Figure 3 shows the plot of $\ln([M]_0/[M])$ vs t . The plot is linear, indicating the stationarity required by eq 14 to hold. From the slope of the linear line, we have $K = 1.7 \times 10^{-10}$ M. Incidentally, Lacroix-Desmazes et al.³¹ have determined K of the same system by the same method in the temperature range from 115 to 130 °C. This temperature range is not wide enough to allow an accurate estimate of K at 80 °C, but these data suggests a K value of about 2.2×10^{-10} M at 80 °C. Tordo et al.⁶ also reported a value of K at 120 °C ($K = 6.0 \times 10^{-9}$ M).

To estimate k_t (at 80 °C), we carried out the polymerization of styrene with [P₀-X]₀ = 25 mM and [BPO]₀ = 4.7 mM. The first-order plot is given in Figure 4 (square symbols). The plot is approximated by a linear relation (dotted line), as required by eq 15, and the slope of the line gives $k_t = 3.0 \times 10^8$ M⁻¹ s⁻¹. This k_t value

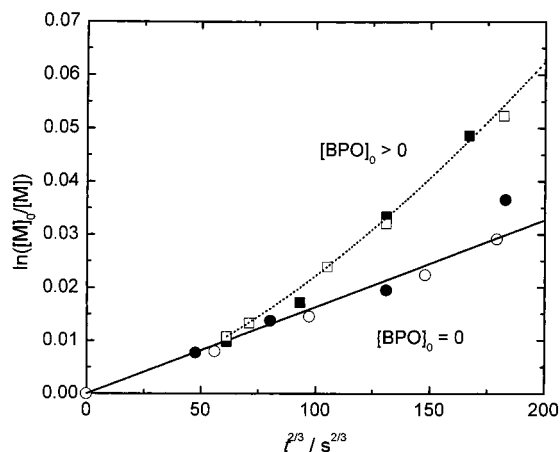


Figure 5. Plot of $\ln([M]_0/[M])$ vs $t^{2/3}$ for the styrene/PS-DEPN(P_0 -X) system (80 °C): $[P_0-X]_0 = 25$ mM. The experiment was duplicated (●, ○). The solid line shows eq 13 with the independently determined rate constants (Table 1). The data points in Figure 4 (■, □) are replotted against $t^{2/3}$. (The dotted line is the reproduction of the one in Figure 4 in the $t^{2/3}$ plot.)

should be understood as a certain mean value applicable to the molecular weight range related to the present experiments (about 3000 ± 1000). The Hui and Hamielec data³⁷ on $k_p/k_t^{1/2}$ combined with the mentioned k_p value gives $k_t = 2.5 \times 10^8 \text{ M}^{-1} \text{ s}^{-1}$. The same k_t value as this was recently reported by Buback et al.,⁴⁰ who used the pulsed laser polymerization (PLP) technique. This agreement is perhaps accidental, since k_t depends on chain length, and these two k_t values refer to different averages over highly polydisperse species. The chain-length dependence of k_t has been studied by several authors,^{41–43} but those results cannot be applied to the present analysis due to different temperature, pressure, and/or chain-length regime. Above all, particular care should be taken of the chain-length regime. All the experimental studies described above refer to degrees of polymerization x_n larger than about 100, and according to the reported results, the maximum possible value of k_t (for $x = 1$) is equal to or smaller than about $2.7 \times 10^8 \text{ M}^{-1} \text{ s}^{-1}$. On the other hand, the k_t between phenylethyl radicals, a unimer model of polystyryl radical, is as large as $1.9 \times 10^9 \text{ M}^{-1} \text{ s}^{-1}$ (25 °C).⁴⁴ This indicates that in the short-polymer regime ($1 < x_n < 100$), with which our analysis is concerned, the chain-length dependence of k_t is particularly strong and thus different from that in the polymer regime. A very recent PLP result shows this explicitly.⁴⁵ For this reason, we consider the difference between the Buback value of k_t (2.5×10^8) and ours (3.0×10^8) is significant. This issue needs more detailed experimental work.

Comparison of Theory and Experiment. To test the rate equations 13 ($R_i = [X^*]_0 = 0$), we heated the mixture of styrene and the PS-DEPN adduct ($[P_0-X]_0 = 25$ mM) at 80 °C for less than 1 h. As will be justified later, the thermal polymerization in this time range is perfectly negligible, so that eq 13 is applicable. Figure 5 shows the comparison of the theory (solid curve) and the duplicated experiment (open and filled circles). The experimental points are well reproduced by the $t^{2/3}$ -dependent linear line predicted by the theory. Thus, the agreement of the theory and experiment is satisfactory on an absolute scale. The experimental data presented by Lutz et al.²⁸ and by Fischer et al.¹⁷ do give additional support for the power law in the same system even at

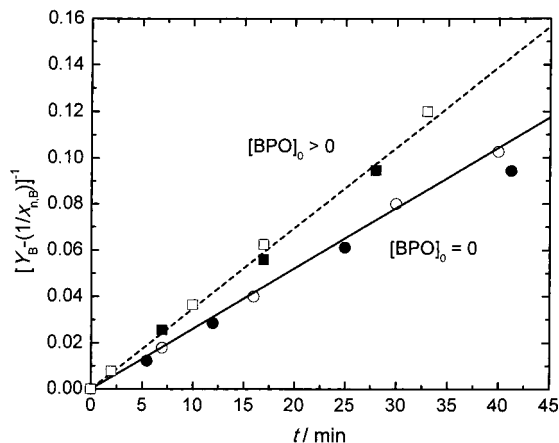


Figure 6. Plot of $[Y_B - (1/x_{n,B})]^{-1}$ vs t for the styrene/PS-DEPN(P_0 -X)/(BPO) systems (80 °C): $[P_0-X]_0 = 25$ mM; $[BPO]_0 = 0$ (●, ○) and 4.7 mM (■, □). The solid and broken lines show eqs 20 and 23, respectively, with the independently determined k_d value (Table 1).

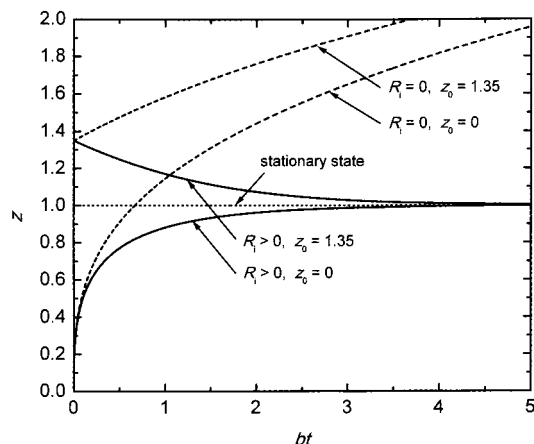


Figure 7. Plot of z vs bt . The solid lines show eq 8 (for $R_i > 0$), and the broken lines show eq 25 (for $R_i = 0$). The dotted line represents the stationary state ($z = 1$).

quite large conversions, even though they do not test the theory on an absolute scale.

Figure 6 shows the comparison of the polydispersity equations 20 (solid line) and 23 (broken line) with the experiments related to Figure 5 (circles) and Figure 4 (squares). In both cases, nearly quantitative agreement of the theory and experiment is noteworthy. This is the first experimental verification of the “highering” of polydispersity caused by the time-dependent concentration of the persistent radical, which is the origin of the characteristic power-law behavior of the conversion factor (eq 13 and Figure 5). The conventional initiation not only accelerates polymerization but also lowers the polydispersity by making $[X^*]$ and hence $[P^*]$ stationary, as was evidenced in Figures 4–6.

Justification of the Experimental Conditions and the Analytical Equations. Finally, the propriety of the experimental conditions and the analytical equations used above is discussed. Figure 7 shows the plot of z vs bt according to eq 8 (solid curves). These are for $R_i > 0$. When $R_i = 0$, we should use eq 11 which can be rewritten

$$z^3 = z_0^3 + \frac{3}{2}bt \quad (R_i = 0) \quad (25)$$

with z , z_0 , and b as defined previously (eqs 9 and 10). Equation 25 is also plotted in Figure 7 (broken curves),

which allows comparison of the reduced concentration z 's of the persistent radicals for $R_i > 0$ and $R_i = 0$. (Even though the parameters b and z for $R_i = 0$ are of unclear physical meaning by themselves, the ratio of the ordinate values at a given reduced time bt gives the ratio of z 's or $[X^*]$'s at that time.)

The above-noted experiment with $[BPO]_0 = 4.7$ mM gives $b = 5 \times 10^{-3} \text{ s}^{-1}$, with which the experiments given in Figure 4 is calculated to be in the range $2.3 < bt < 11$. Figure 7 indicates that the stationary state should be achieved in this time range. In the experiment without BPO, there still exists thermal initiation, which amounts to $b = 2 \times 10^{-6} \text{ s}^{-1}$. The time range of the experiments given in Figure 5 corresponds to $bt < 0.005$, where the thermal initiation is entirely negligible, as Figure 7 indicates (compare the curves for $R_i > 0$ and $R_i = 0$). Furthermore, the experiment with $[X^*]_0 = 1.8$ mM corresponds to $z_0 = 1.35$. The thermal initiation amounts to $bt = 0.07$ after the 10 h experiment given in Figure 3. Again, Figure 7 suggests that the change of z and hence of $[X^*]$ is trivial in this time range, and the system may be regarded as being in a stationary state.

Regarding the polydispersity argument related to the experiment with BPO (the broken curve in Figure 6), we should note that it took about 10 min to reach the stationary state. Since the prestationary history is recorded on the polydispersity of the polymer, this effect has to be somehow corrected for. A sufficient correction can be done by regarding the time relevant to the first (smallest t) data point in the stationary state as $t = 0$ and the polymer corresponding to this point as an initiating adduct A (cf. eq 17 and the following remarks). The data points given in Figure 6 (squares) were in fact obtained in this way. For details of the GPC analysis of this kind, the readers are referred to ref 24.

In this work, we have limited the experimental time range (conversion range) to an extremely low one, as was necessary to observe the theoretically predicted behavior in a strict sense. We should also note that all the analytical equations used in this work (eqs 8, 13, 14, 15, 20, and 23) have been confirmed to agree, with negligible errors, with the (rigorous) solutions obtained by numerically solving the differential equations without introducing the quasi-equilibrium assumption.^{19,46,47}

Conclusions

The kinetic theories on the DC type LRP were comprehensively tested by experiments for the styrene/DEPN systems at 80 °C. For the system with no (negligible) conventional initiation, the experiments quantitatively agreed with the theories with respect to both the polymerization rate and polydispersity. It was also experimentally demonstrated for the first time that the conventional initiation can not only increase the conversion but also lower the polydispersity at a fixed polymerization time, as the theories predict. It is highly unlikely that kinetic parameters such as k_p and k_t in LRP at all differ from those in conventional FRP, insofar as the nitroxide-mediated LRP is concerned.

Acknowledgment. We thank Professor H. Fischer for his interest in this work and sending his numerical solutions (obtained by the use of Matlab I), which generally showed excellent agreement with the analytical solutions and hence with the experiments presented in this work. This work was supported by Grants-in-

Aid for Scientific Research, the Ministry of Education, Culture, Sports, Science and Technology, Japan (Grants-in-Aid 12450385 and 12555260).

References and Notes

- (1) (a) Matyjaszewski, K., Ed. *ACS Symp. Ser.* **1998**, 685; **2000**, 768. (b) Matyjaszewski, K., Davis, T. P., Eds.; *Handbook of Radical Polymerization*; John Wiley & Sons: New York, in press.
- (2) Solomon, D. H.; Rizzardo, E.; Cacioli, P. Eur. Pat. Appl. EP135280 (Chem. Abstr. **1985**, 102, 221335q).
- (3) Georges, M. K.; Veregin, R. P. N.; Kazmaier, P. M.; Hamer, G. K. *Macromolecules* **1993**, 26, 2987.
- (4) Grimaldi, S.; Lemoigne, F.; Finet, J. P.; Tordo, P.; Nicol, P.; Plechot, M. WO 96/24620.
- (5) Benoit, D.; Chaplinski, V.; Braslau, R.; Hawker, C. J. *J. Am. Chem. Soc.* **1999**, 121, 3904.
- (6) Benoit, D.; Grimaldi, S.; Robin, S.; Finet, J. P.; Tordo, P.; Gnanou, Y. *J. Am. Chem. Soc.* **2000**, 122, 5929.
- (7) Perkins, M. J. *J. Chem. Soc.* **1964**, 5932.
- (8) Fischer, H. *J. Am. Chem. Soc.* **1986**, 108, 3925.
- (9) Ruegge, D.; Fischer, H. *Int. J. Chem. Kinet.* **1989**, 21, 703.
- (10) Daikh, B. E.; Finke, R. G. *J. Am. Chem. Soc.* **1992**, 114, 2938.
- (11) Jonhson, C. H. J.; Moad, G.; Solomon, D. H.; Spurling, T. H.; Vearring, D. *J. Aust. J. Chem.* **1990**, 43, 1215.
- (12) Fukuda, T.; Terauchi, T.; Goto, A.; Ohno, K.; Tsujii, Y.; Miyamoto, T.; Kobatake, S.; Yamada, B. *Macromolecules* **1996**, 29, 6396.
- (13) Greszta, D.; Matyjaszewski, K. *Macromolecules* **1996**, 29, 7661.
- (14) Veregin, R. P. N.; Georges, M. K.; Hamer, G. K.; Kazmaier, P. M. *Macromolecules* **1995**, 28, 4391.
- (15) Fischer, H. *Macromolecules* **1997**, 30, 5666.
- (16) (a) Fischer, H. *J. Polym. Sci., Part A: Polym. Chem.* **1999**, 37, 1885. (b) Souaille, M.; Fischer, H. *Macromolecules* **2000**, 33, 7378. (c) Souaille, M.; Fischer, H. *Macromolecules* **2002**, 35, 248.
- (17) Fischer, H. *Chem. Rev.* **2001**, 101, 3581.
- (18) Fukuda, T.; Goto, A. *ACS Symp. Ser.* **2000**, 768, 27.
- (19) Fukuda, T.; Goto, A.; Tsujii, Y. In *Handbook of Radical Polymerization*; Matyjaszewski, K., Davis, T. P., Eds.; John Wiley & Sons: New York, in press.
- (20) Fukuda, T.; Goto, A.; Ohno, K. *Macromol. Rapid Commun.* **2000**, 21, 151.
- (21) Ohno, K.; Tsujii, Y.; Miyamoto, T.; Fukuda, T.; Goto, M.; Kobayashi, K.; Akaike, T. *Macromolecules* **1998**, 31, 1064.
- (22) Fukuda, T.; Terauchi, T. *Chem. Lett.* **1996**, 293.
- (23) (a) Goto, A.; Fukuda, T. *Macromolecules* **1997**, 30, 4272. (b) Tanaka, T.; Omoto, M.; Inagaki, H. *J. Macromol. Sci., Phys.* **1980**, B17, 211.
- (24) Fukuda, T.; Goto, A. *Macromol. Rapid Commun.* **1997**, 18, 683.
- (25) Goto, A.; Fukuda, T. *Macromol. Chem. Phys.* **2000**, 201, 2138.
- (26) Goto, A.; Fukuda, T. *Macromolecules* **1997**, 30, 5183.
- (27) Greszta, D.; Matyjaszewski, K. *Macromolecules* **1996**, 29, 5239.
- (28) Lutz, J.-F.; Lacroix-Desmazes, P.; Boutevin, B. *Macromol. Rapid Commun.* **2001**, 22, 189.
- (29) Bon, A. F.; Bosveld, M.; Klumperman, B.; German, A. L. *Macromolecules* **1997**, 30, 324.
- (30) Benoit, D.; Hawker, C. J.; Huang, E. E.; Lin, Z.; Russell, T. P. *Macromolecules* **2000**, 33, 1505.
- (31) Lacroix-Desmazes, P.; Lutz, J.-F.; Boutevin, B. *Macromol. Chem. Phys.* **2000**, 201, 662.
- (32) Lacroix-Desmazes, P.; Lutz, J.-F.; Chauvin, F.; Severac, R.; Boutevin, B. *Macromolecules* **2001**, 34, 8866.
- (33) Matyjaszewski, K.; Patten, T. E.; Xia, J. *J. Am. Chem. Soc.* **1997**, 119, 674.
- (34) Matyjaszewski, K.; Kajiwar, A. *Macromolecules* **1998**, 31, 548.
- (35) Matyjaszewski, K.; Miller, P. J.; Shukla, N.; Immaraporn, B.; Gelman, A.; Luokala, B. B.; Garoff, S.; Siclován, T.; Kickelbick, G.; Vallant, T.; Hoffmann, H.; Pakula, T. *Macromolecules* **1999**, 32, 8716.
- (36) Zhang, H.; Klumperman, B.; Ming, W.; Fischer, H.; van der Linde, R. *Macromolecules* **2001**, 34, 6169.
- (37) Hui, A. W.; Hamielec, A. E. *J. Appl. Polym. Sci.* **1972**, 16, 749.
- (38) Molnar, S. *J. Polym. Sci., Part A-1* **1972**, 10, 2245.

- (39) Gilbert, R. G. *Pure Appl. Chem.* **1996**, 68, 1491.
- (40) Buback, M.; Kuchta, F.-D. *Macromol. Chem. Phys.* **1997**, 198, 1455. The $2k_t$ in this reference corresponds to the k_t in the present paper.
- (41) Mahabadi, H.-K. *Macromolecules* **1991**, 24, 606.
- (42) Olaj, O. F.; Vana, P. *Macromol. Rapid Commun.* **1998**, 19, 433.
- (43) Buback, M.; Busch, M.; Kowollik, C. *Macromol. Theory Simul.* **2000**, 9, 442.
- (44) Sobek, J.; Martschke, R.; Fischer, H. *J. Am. Chem. Soc.* **2001**, 123, 2849.
- (45) de Kock, J. B. L.; van Herk, A. M.; German, A. L. *J. Macromol. Sci., Polym. Rev.* **2001**, C41, 199.
- (46) Tsujii, Y.; Yoshikawa, C.; Goto, A.; Fukuda, T., to be published.
- (47) Fischer, H., private communication.

MA012203T